

1 Black carbon aerosol in winter northeastern Qinghai-Tibetan
2 Plateau, China: [the source, mixing state and optical property](#)

3 **Q. Y. Wang¹, R.-J. Huang^{1,2,3}, J. J. Cao^{1,5}, X. X. Tie¹, H. Y. Ni¹,**
4 **Y. Q. Zhou¹, Y. M. Han¹, T. F. Hu¹, C. S. Zhu¹, T. Feng^{4,5}, N.**
5 **Li⁶, J. D. Li¹**

6 [1] Key Laboratory of Aerosol Chemistry and Physics, Institute of Earth Environment,
7 Chinese Academy of Sciences, Xi'an 710061, China

8 [2] Laboratory of Atmospheric Chemistry, Paul Scherrer Institute (PSI), 5232 Villigen,
9 Switzerland

10 [3] Centre for Climate and Air Pollution Studies, Ryan Institute, National University of
11 Ireland Galway, University Road, Galway, Ireland

12 [4] School of Human Settlements and Civil Engineering, Xi'an Jiaotong University, Xi'an
13 710054, China

14 [5] Institute of Global Environmental Change, Xi'an Jiaotong University, Xi'an 710049,
15 China

16 [6] National Taiwan University, Department of Atmospheric Science, Taipei 10617, Taiwan

17

18 Correspondence to: R.-J. Huang (rujin.huang@ieecas.cn) or J. J. Cao (cao@loess.llqg.ac.cn)

19

20 **Abstract**

21 Black carbon (BC) aerosol at high-altitude Qinghai-Tibetan Plateau has potential effects on
22 the regional climate and hydrological cycle. An intensive measurement campaign was
23 conducted at Qinghai Lake (~3200 [ASLmetres above sea level](#)) at the edge of the northeastern
24 Qinghai-Tibetan Plateau during winter using a ground-based single particle soot photometer
25 (SP2) and a photoacoustic extinctions (PAX). The average [concentration of refractory BC](#)
26 [\(rBC\)-concentration](#) and number fraction of coated [rBC](#) were found to be $160 \pm 190 \text{ ng m}^{-3}$
27 and 59.3% for the entire campaign, respectively. Significant enhancements of [rBC](#) loadings

1 and number fraction of coated rBC were observed during pollution episode, with an average
2 value of 390 ng m^{-3} and ~~64.665~~%, respectively. The mass size distribution of rBC particles
3 showed lognormal distribution with a peak diameter of $\sim 187 \text{ nm}$ regardless of the pollution
4 level. Five-day backward trajectory analysis ~~combined with the fire counts map~~ suggests that
5 the ~~biomass burning~~ air masses from North India contributed ~~ed~~ to the increased rBC loadings
6 during the campaign. The potential source contribution function (PSCF) model combined
7 with the fire counts map further proves that biomass burning from North India is an important
8 potential region-source influencing northeastern Qinghai-Tibetan Plateau during the pollution
9 episode. The rBC mass absorption cross section (MAC_{rBC}) at $\lambda = 532 \text{ nm}$ was slightly larger
10 in clean days ($14.9 \text{ m}^2 \text{ g}^{-1}$) than during pollution episode ($9.3 \text{ m}^2 \text{ g}^{-1}$), likely due to the effects
11 of brown carbon and the uncertainty of the MAC_{rBC} calculation. The MAC_{rBC} was positively
12 correlated with number fraction of coated rBC during pollution episode with an increasing
13 rate of $0.18 (\text{m}^2 \text{ g}^{-1}) \%^{-1}$. The number fraction of coated rBC particles showed positive
14 correlation with light absorption, suggesting that the increase of coated rBC particles will
15 enhance the light absorption. Compared to rBC mass concentration, rBC mixing sate is more
16 important in determining absorption during pollution episode, estimated from the same
17 percentagewise increment of either rBC mass concentration or the number fraction of coated
18 rBC . The estimated BC direct radiative forcing was $+0.93 \text{ W m}^{-2}$ for pollution episode, which
19 is 2 times larger than that in clean days. Our study provides insight into the potential climatic
20 impacts of rBC aerosol transported to the Qinghai-Tibetan Plateau from South Asian regions,
21 and is also useful for future modeling studies.

23 1 Introduction

24 Black carbon (BC) aerosol has received worldwide concern due to its effects on climate and
25 human health (Anenberg et al., 2012; Bond et al., 2013). BC shows an overall warming effect
26 by either absorbing incoming solar radiation in the atmosphere or by reducing the albedo of
27 surface (i.e., snow and ice) (Jacobson, 2001; Ramanathan and Carmichael, 2008; Kühn et al.,
28 2014). A total climate forcing of BC particles is estimated to be $+1.1 \text{ W m}^{-2}$, which is ranked
29 as the second largest contributor to anthropogenic radiative forcing after carbon dioxide in the
30 present-day atmosphere (Bond et al., 2013). BC particles, derived from incomplete
31 combustion of fossil fuels or biomass, are mainly hydrophobic when emitted, but become
32 hygroscopic over time due to atmospheric aging processes (Cheng et al., 2006; 2012). When

1 BC particles are mixed with water-soluble aerosol composition, they can serve as cloud
2 condensation nuclei and therefore affect microphysical properties of clouds leading to indirect
3 effect on climate ([Hansen et al., 2005](#); Lohmann and Feichter, 2005; [Riemer et al., 2010](#); [Rose](#)
4 [et al., 2011](#)). [BC also shows semi-direct effect through interaction with cloud processes \(Koch](#)
5 [and Del Genio, 2010\)](#). Moreover, the impacts of BC aerosols on the radiative balance may
6 lead to far-reaching consequences, such as global dimming (Wild et al., 2007), lower crop
7 yields (Tollefsen et al., 2009), and negative impacts on terrestrial and aquatic ecosystems
8 (Forbes et al., 2006).

9 The Qinghai-Tibetan Plateau is known as the “Third Pole” of the Earth because of its
10 immense area and high elevation. It covers the area of 27–45 °N, 70–105 °E with an average
11 elevation >4000 m ASL (above sea level). Due to the special landform, ecosystem and
12 monsoon circulation, the Qinghai-Tibetan Plateau exerts profound effects on regional and
13 global radiative budget and climate (Kopacz et al., 2011; Su et al., 2013; Yang et al., 2014).
14 The Qinghai-Tibetan Plateau is surrounded by many important anthropogenic BC aerosol
15 source areas (Zhang et al., 2009), such as South Asia (e.g., India) and East Asia (e.g., China).
16 Inventory study suggests that the BC emissions in China and India have increased by 40%
17 and 54% from 2000 to 2008, respectively (Kurokawa et al., 2013). Due to the general
18 circulation patterns, the Qinghai-Tibetan Plateau becomes a strong receptor of these high BC
19 source areas (Cao et al., 2010; Xia et al., 2011; Cong et al., 2013; Zhao et al., 2013). Lu et al.
20 (2012) shows that South Asia and East Asia are the main source regions, accounting for 67%
21 and 17% of BC transported to the Himalayas and Qinghai-Tibetan Plateau on an annual basis,
22 followed by former USSR (~8%), Middle East (~4%), Europe (~2%), and Northern Africa
23 (~1%). Deposition of BC on snow and ice at the Qinghai-Tibetan Plateau would decrease the
24 snow surface albedo (Xu et al., 2012; Ming et al., 2013). The Qinghai-Tibetan Plateau
25 Glaciers, which are the largest glaciers outside of the Polar Regions, have shown signs of
26 retreat (Xu et al., 2009). The snowmelt from Qinghai-Tibetan Plateau vitally affects the
27 sustaining seasonal water availability leading to agriculture security in South, East, and
28 Southeast Asia (Immerzeel et al., 2010).

29 The effect of BC transported from surroundings on Qinghai-Tibetan’s environment and
30 climate is of great significance. However, BC studies are still very scarce to date in the
31 Qinghai-Tibetan Plateau (e.g., Cao et al., 2010; Zhao et al., 2013; Wang et al., 2014a). In
32 these limited studies, online and offline filter-based techniques are often used. Due to inherent

1 systematic limitations, direct examination of BC size distribution and mixing state with filter-
2 based measurements is not feasible (Watson et al., 2005; Slowik et al., 2007; Collaud Coen et
3 al., 2010; Bond et al., 2013). The BC optical properties are dependent on its physical (e.g.,
4 size and shape) and chemical (e.g., mixing with other materials) features. For example, the
5 degree of enhancement in mass absorption cross section from internal mixture of BC with
6 other aerosol components can lead to large difference in the prediction of global radiative
7 budget (Bond et al., 2006; Chung et al., 2012; Zhuang et al., 2013). Consequently, accurate
8 characterization of BC particles is crucial for a precise estimate of the impacts of BC on the
9 atmospheric radiative forcing, human health, and air quality. In this study, a single particle
10 soot photometer (SP2) and a photoacoustic extinctions (PAX) were used to investigate the
11 [refractory black carbon \(rBC\)](#) mass concentrations, size distribution, mixing state, and aerosol
12 light absorption properties in northeastern Qinghai-Tibetan Plateau. The primary objectives of
13 this study were (1) to investigate the important potential [rBC](#) source regions responsible for
14 the high wintertime [rBC](#) concentration in the Northeastern Qinghai-Tibetan Plateau, (2) to
15 study the effect of [rBC](#) mixing state on light absorption properties, (3) to estimate the direct
16 radiative forcing during [rBC](#) pollution episode.

17 **2 Methodology**

18 **2.1 Measurement site**

19 Qinghai Lake (36.53–37.25 °N and 99.6–100.78 °E), the largest saline lake in China, is
20 located ~3200 m ASL in a drainage closed intermountain basin on the Northeast Qinghai-
21 Tibetan Plateau with an area of ~4400 km² (Figure 1). This region is highly sensitive to global
22 climate change, because it is situated in the sensitive semi-arid zone between the Asian
23 monsoon-controlled area and the westerly jet stream-influenced area (An et al., 2012).
24 Intensive measurements were taken from 16–27 November, 2012 from the rooftop (~15 m
25 above ground level) of a sampling tower at the “Bird Island” peninsula (36.98 °N, 99.88 °E),
26 which is located at the northwest section of the Qinghai Lake shore as shown in Figure 1.

27 **2.2 [rBC](#) mass and mixing state measurements**

28 The commercially available SP2 instrument (Droplet Measurement Technology, Boulder, CO,
29 USA) has proven useful for measuring [rBC](#) mass, size, and mixing state (e.g., Gao et al., 2007;
30 Moteki and Kondo, 2007; Schwarz et al., 2010; Wang et al., 2015). The operating principles

1 of the SP2 are described elsewhere (Stephens et al., 2003; Schwarz et al., 2006). Briefly, the
2 SP2 relies on laser-induced incandescence to quantify the r_{BC} mass of individual particles.
3 Continuous intracavity Nd:YAG laser light at 1064 nm is used to heat r_{BC} -containing
4 particles to their vaporization point. The peak incandescence signal is linearly related to the
5 r_{BC} mass in the particle irrespective of the particle morphology or mixing state; this holds
6 true over most of the r_{BC} mass range typically observed in the accumulation mode (Slowik et
7 al., 2007). In this work, the r_{BC} mass in the range of ~ 0.4 – 1000 fg, equivalent to ~ 70 – 1000
8 nm volume equivalent diameter (VED), is quantified, assuming a void-free density of 2.0 g
9 cm^{-3} (Schwarz et al., 2008). This range covers $>90\%$ of the r_{BC} mass in the accumulation
10 mode. The incandescence signal was calibrated using a standard fullerene soot sample (Lot
11 F12S011, Alpha Aesar, Inc., Ward Hill, Massachusetts). The total uncertainty in the r_{BC}
12 mass determination was $\sim 25\%$. More details about the SP2 calibration and uncertainty can be
13 found in our previous work (Wang et al., 2014a). Note that the SP2 only quantifies the most
14 refractory and most efficient light-absorbing component of combustion aerosol. The r_{BC}
15 concentration is adjusted to standard temperature and pressure (STP, $T_{\text{standard}} = 273.15$ K and
16 $P_{\text{standard}} = 1013.25$ hPa).

17 The SP2 is capable of determining the r_{BC} mixing state. The time delay between the peaks
18 from the scattered light and incandescence signals is an indicator of the amount of non- r_{BC}
19 material mixed internally with individual r_{BC} particles (Schwarz et al., 2006; McMeeking et
20 al., 2011; Perring et al., 2011; Wang et al., 2014a). This method is sensitive to optically
21 significant amounts of non- r_{BC} material. The time delay occurs because the coatings must be
22 removed from the r_{BC} particle before the onset of incandescence. Because the scattering
23 measurement is rather noisy for small particles and become saturation for large particles, the
24 mixing state was studied for r_{BC} core between ~ 70 and ~ 275 nm VED, which constitute the
25 majority of r_{BC} particle numbers (Wang et al., 2014a). The limitation of SP2 instrument is
26 discussed in Taylor et al. (2015) when considering leading-edge scattering. The number
27 fraction of coated r_{BC} particles which is calculated from the distribution of time delay is an
28 indicator of the degree to which the r_{BC} particles are coated with other substances. This
29 number fraction is higher for more aged r_{BC} particles due to the formation of coating from
30 atmospheric physical and chemical processes including coagulation, condensation, and
31 heterogeneous reactions (Liu et al., 2013; Browne et al., 2015).

2.3 Particle light absorption measurements

The PAX (Droplet Measurement Technology, Boulder, CO, USA) measures light absorption and scattering coefficients simultaneously using a modulated diode laser. The light absorption coefficient is measured based on the intracavity photoacoustic technology. A laser beam in the acoustic chamber of the instrument heats suspended absorbing particles, by which a pressure wave is produced and detected with a sensitive microphone. A wide-angle integrating reciprocal nephelometer in the acoustic chamber measures the light scattering coefficient regardless of the particles' chemical makeup, mixing state, or morphology. In this study, the light absorption at $\lambda = 532$ nm is measured. Before sampling, nitrogen dioxide (NO_2) and ammonium sulfate are used for the calibration of light absorption and scattering, respectively. The PAX can provide the light extinction coefficient independently using the laser power. NO_2 was used to produce an absorption reading of $\sim 500\text{--}30000$ Mm^{-1} . A correction factor was then established from the relationship between the calculated light extinction coefficient using laser power and the measured light absorption. The uncertainty of the PAX is estimated to be $\sim 10\%$. Like SP2 measurement, the absorption measurement reported here is also corrected for the standard temperature and pressure.

3 Results and discussion

3.1 Mass, size and mixing state of rBC aerosol

The time series of hourly averaged rBC mass concentrations and the mixing state obtained during the campaign are shown in Figure 2, and a statistical summary of the data is presented in Table 1. The mean concentration of rBC aerosol (\pm standard deviation) was 160 ± 190 ng m^{-3} during the entire campaign period, ranging from 6 ng m^{-3} to 1040 ng m^{-3} . The mean number fraction of coated rBC is found to be $59.3 \pm 76.9\%$ (range $39.840\text{--}73.2\%$), suggesting the majority of aged rBC particles in wintertime in the Qinghai Lake region. It is found that $\sim 3025\%$ of the rBC values are higher than the mean-75th value, and the variation coefficient (defined by SD/mean) of rBC values reaches as high as 120%, suggesting a large rBC burden even at the free tropospheric altitude. ~~It is found that $\sim 30\%$ of the BC values are higher than the mean value, and the variation coefficient (defined by SD/mean) of BC values reaches as high as 120%, suggesting a large BC burden even at the free tropospheric altitude.~~ Elevated rBC concentration was observed from 19 to 21 November (defined as a pollution episode hereafter) with an average rBC loading of 390 ng m^{-3} , which is about 4 times higher than that

1 from the rest of measurement period (86 ng m^{-3} , defined as clean days). The mean number
2 fraction of coated rBC also increases to 64.665% during the pollution episode, higher than
3 that in the clean days (57.758%). Given that local rBC emissions in the Qinghai Lake region
4 and even the entire Qinghai-Tibetan Plateau are very limited, the enhanced rBC
5 concentrations observed during this campaign are most likely from regional transport as
6 discussed below.

7 Figure 3 shows the mass size distribution of rBC particles for the entire campaign period. A
8 lognormal size distribution pattern in VED for the size of rBC core of a particle is found, with
9 a very close peak diameter for rBC pollution episode (188 nm) and clean days (187 nm). The
10 size distributions of rBC core in the ambient atmosphere are affected by the size of fresh rBC
11 particles and the subsequent atmospheric processing (Bond et al., 2013). The growth of rBC
12 particles is a complex process, including water accretion, coagulation, condensation, and the
13 accumulation of other materials through heterogeneous reactions. However, only the process
14 of coagulation can lead to the increase of rBC core in VED. The coagulation of particles in
15 ambient air is dominated by Brownian motion, a slow process for particles in the
16 accumulation mode (Seinfeld and Pandis, 1998). Therefore, the similarity in VED size
17 distribution for rBC core between clean and pollution episode indicates that the measured rBC
18 particles are likely from biomass burning emissions, given that fossil fuel and biomass
19 burning tend to have different rBC size distributions and that the peak diameter measured in
20 this study is similar to the reported rBC peak diameter from biomass burning plumes (range
21 $\sim 187\text{--}193 \text{ nm}$, see Kondo et al., 2011; Sahu et al., 2012; Taylor et al., 2014).

22 3.2 rBC potential pollution source areas

23 To examine the contribution of regional rBC transport, five-day back trajectories were
24 calculated using the hybrid single-particle Lagrangian integrated trajectories (HYSPLIT)
25 model (<http://ready.arl.noaa.gov/HYSPLIT.php>~~www.arl.noaa.gov/reday.html~~). The HYSPLIT
26 model was driven with full vertical dynamics using gridded meteorological data (Global Data
27 Assimilation System, GDAS1). ~~was used to compute the five-day back trajectories using BC~~
28 ~~as a marker. The five-day period is chosen because the atmospheric lifetime of BC is typically~~
29 ~~in the order of one week (Chung and Seinfeld, 2005; Cape et al., 2012).~~ Figure 4a shows the
30 hourly results of backward trajectories calculated with the arrival height of 100, 500 and 1000
31 m above ground level. The rBC data were averaged to 1 hr in order to match the timestep of
32 the trajectories. The different arrival height of trajectories shows similar transport directions,

1 ~~suggesting the air masses mixed well at different altitude.~~ During \underline{r} BC pollution episode, the
2 air masses were mainly originated from the regions of high \underline{r} BC emissions in North India
3 (Sahu et al., 2008), which then passed over the rather clean western Qinghai-Tibetan Plateau
4 (Zhang et al., 2009). In contrast, the air masses were originated from Europe and passed
5 through the western part of China during clean days. ~~An aerosol optical depth (AOD) map,~~
6 ~~retrieved from the measurements of Moderate Resolution Imaging Spectroradiometer~~
7 ~~(MODIS) on the Terra satellite, describes the mean atmospheric aerosol loading around~~
8 ~~Qinghai-Tibetan Plateau (Figure 5a). Since 5-day back trajectory analysis shows that the~~
9 ~~polluting air masses arriving the measurement site on 19–21 November were from North~~
10 ~~India, the pollution status of North India on 14–16 November (i.e., 5 days backward) was~~
11 ~~examined. As shown in Figure 5a, high AOD values can be found along the Indo-Gangetic~~
12 ~~Basin in India and South Pakistan, indicating heavy pollution in this region. The fire counts~~
13 ~~map obtained from MODIS observation on NASA satellites also shows a large number of~~
14 ~~biomass burning activities in North India during 14–16 November, indicating large biomass~~
15 ~~burning aerosol (including BC aerosol) emissions. Although the high altitude of the~~
16 ~~Himalayas was thought to be a physical wall for atmospheric pollutants, previous studies~~
17 ~~indicate that the high Himalayan valleys can act as a “direct channel” for the transport of air~~
18 ~~pollutants up to 5000 m ASL (e.g., Bonasoni et al., 2010). After reaching the north of the~~
19 ~~Himalayan, the air pollutants can further transport to the central Qinghai-Tibetan Plateau~~
20 ~~(Hindman and Upadhyay, 2002; Xia et al., 2011). Therefore, the BC pollution episode~~
21 ~~observed in the Qinghai Lake measurement site is most likely derived from the biomass~~
22 ~~burning emissions in North India.~~

23 The potential source contribution function (PSCF) model (e.g., Wang et al., 2006) was used
24 to further explore the potential source regions which influence \underline{r} BC concentration in the
25 Qinghai Lake region. To do so, the geographic region covered by the trajectories was divided
26 into an array of 0.5×0.5 degree grid cells. The PSCF values for the grid cells were calculated
27 by counting the trajectory segment endpoints that terminate within each cell. The number of
28 endpoints that fall in the ij th cell is designated as n_{ij} . The number of endpoints for the same
29 cell corresponding to \underline{r} BC concentrations higher than an arbitrarily set criterion is defined to
30 be m_{ij} . Then, the PSCF value for the ij th cell is defined as: $PSCF_{ij}=m_{ij}/n_{ij}$. Because of the
31 impact of small values of n_{ij} , an arbitrary weight function W_{ij} was used to better reflect the
32 uncertainty in the values for these cells (Polissar et al., 1999). The weight function reduces the
33 PSCF values when the total number of the endpoints in a particular cell is less than about

1 three times the average value of the end points per each cell. Here, W_{ij} is defined as (Polissar
2 et al., 2001):

$$3 \quad W_{ij} = \begin{cases} 1.00 & 80 < n_{ij} \\ 0.70 & 20 < n_{ij} \leq 80 \\ 0.42 & 10 < n_{ij} \leq 20 \\ 0.05 & n_{ij} \leq 10 \end{cases} \quad (1)$$

4 Although PSCF model is often used to determine the potential source regions (e.g., Wang
5 et al., 2006; Heo et al., 2013; Zhang et al., 2013), a limitation of this model is that grid cells
6 can have the same PSCF value when sample concentrations at the receptor site are either only
7 slightly higher or extremely higher than the criterion. This may lead to difficulties in
8 distinguishing moderate sources from strong ones. To compensate for this limitation, the
9 PSCF result calculated from the 75th percentile of all the data is set as the criterion (170 ng m^{-3})
10 ³) in this study. Figure 4b shows the map of PSCF results for the entire campaign period. High
11 PSCF values are found at North India. The PSCF values are low in the Qinghai Lake and
12 surrounding regions, indicating lower likelihood of high rBC emissions from local sources
13 compared to regional transport from North India. An aerosol optical depth (AOD) map,
14 retrieved from the measurements of Moderate Resolution Imaging Spectroradiometer
15 (MODIS) on the Terra satellite, describes the mean atmospheric aerosol loading around
16 Qinghai-Tibetan Plateau (Figure 5a). High AOD values can be found along the Indo-Gangetic
17 Basin in India and South Pakistan, indicating heavy pollution in this region. The fire counts
18 map (Figure 5b) obtained from MODIS observation on NASA satellites also shows a large
19 number of biomass burning activities in North India, indicating large biomass burning aerosol
20 (including rBC aerosol) emissions. Although the high altitude of the Himalayas was thought
21 to be a physical wall for atmospheric pollutants, previous studies indicate that the high
22 Himalayan valleys can act as a “direct channel” for the transport of air pollutants up to 5000
23 m ASL (e.g., Bonasoni et al., 2010). After reaching the north of the Himalayan, the air
24 pollutants can further transport to the central Qinghai-Tibetan Plateau (Hindman and
25 Upadhyay, 2002; Xia et al., 2011). Therefore, the rBC pollution episode observed in the
26 Qinghai Lake measurement site is most likely derived from the biomass burning emissions in
27 North India.

3.3 Optical properties of rBC aerosol

The hourly light absorption coefficient varied from 0.0 to 18.1 Mm^{-1} with an average value of $2.1 \pm 2.4 \text{ Mm}^{-1}$ for the entire campaign (Figure 2). The average value increased to $3.7 \pm 2.9 \text{ Mm}^{-1}$ during rBC pollution episode, which is ~ 3 times higher than the average value in clean days ($1.3 \pm 1.6 \text{ Mm}^{-1}$). The rBC mass absorption cross section (MAC_{rBC} , expressed here in $\text{m}^2 \text{ g}^{-1}$) is one of the most important optical properties for rBC aerosol because this parameter links optical properties to rBC mass. The MAC_{rBC} can be calculated by dividing the absorption coefficient measured with the PAX by the rBC mass concentration from the SP2 ($MAC_{rBC} = [\text{Absorption}]/[rBC]$). Due to the difference in cutoff size for PAX ($< 2.5 \mu\text{m}$) and for SP2 ($< 1.0 \mu\text{m}$), the MAC_{rBC} may be overestimated by $\sim 13\%$ given that BC concentration in $PM_{1.0}$ accounted for $\sim 85\%$ of $PM_{2.5}$ in the Tibetan Plateau (Wan et al., 2015).

Figure 6a and b show histograms of the MAC_{rBC} values during clean days and pollution episode, respectively. The distribution of MAC_{rBC} in clean days tends to larger values than that during pollution episode, with an average value of $14.9 \pm 8.9 \text{ m}^2 \text{ g}^{-1}$ for clean days and $9.3 \pm 3.1 \text{ m}^2 \text{ g}^{-1}$ for pollution episode. These values are higher than the MAC_{rBC} of $7.8 \text{ m}^2 \text{ g}^{-1}$ for uncoated rBC particles (interpolated to 532 nm from 550 nm assuming an Absorption Ångström Exponent of 1.0) suggested by Bond and Bergstrom (2006). It is interesting that the MAC_{rBC} in clean days is $\sim 60\%$ larger than that during pollution episode, the reason for which is not clear. A possible explanation involves the interference from brown carbon. Previous studies demonstrate that brown carbon, like black carbon, is an important light-absorbing aerosol composition in the atmosphere which can absorb light at visible wavelength (e.g., $\lambda = 532 \text{ nm}$) (Yang et al., 2009). In the rural areas of Qinghai, biofuels including yak and sheep dung, firewood, and crop residues account for $\sim 80\%$ of total household energy (Ping et al., 2011). Biofuel/biomass combustion emissions are considered as especially significant sources for brown carbon (Andreae and Gelencser, 2006). It may produce enough brown carbon (particularly during the smoldering combustion phase) influencing the light absorption when rBC loading is low. Thus, the MAC_{rBC} may be overestimated in clean days. In addition, the calculation method using the light absorption and rBC mass may also introduce uncertainty, especially when rBC concentration is low. The high MAC_{rBC} values always correspond to the very low rBC mass. The MAC_{rBC} calculation method can bring $\sim 30\%$ uncertainty estimated from the square root of uncertainties in the PAX (10%) and SP2 (25%) measurements.

1 To further investigate the effect of rBC mixing state on MAC_{rBC} , the MAC_{rBC} values were
2 plotted against the number fraction of coated rBC. As shown in Figure 7, the MAC_{rBC} was not
3 correlated with the number fraction of coated rBC during clean days, but positive correlation
4 was observed during pollution episode suggesting that the mixing state leads to the increase of
5 the MAC_{rBC} . The slope of $0.18 \text{ (m}^2 \text{ g}^{-1}) \%^{-1}$ obtained from the linear regression is arguably
6 representative of the rate of the mixing state effect on the MAC_{rBC} .

7 Both laboratory studies and field measurements have shown that the BC light absorption
8 (related to its direct radiative effects) can be enhanced by a factor of 1.5–2.0 when BC
9 particles are internally mixed with other non-light-absorbing aerosol components including
10 sulfate, nitrate, organics and water (e.g., Bond et al., 2006; Shiraiwa et al., 2010; Wang et al.,
11 2014b). This is because the non-absorbing materials act like a lens and therefore refract the
12 light toward the absorbing BC core, leading to the enhancement of absorption on visible light.
13 Figure 8 shows the relationship between light absorption and rBC mixing state during clean
14 days and pollution episode. In clean days the light absorption shows no significant correlation
15 with number fraction of coated rBC, which could be attributed to the influences of brown
16 carbon. In contrast, during pollution episodes the light absorption coefficients generally
17 increase with increasing number fraction of coated rBC with the latter being positively
18 correlated with the rBC mass concentration during pollution episode (see Figure 8b). Such
19 correlation indicates that the outflow from polluted south Asia would increase the rBC mass
20 concentration leading to light absorption enhancement on the one hand, and the increased
21 number fraction of coated rBC particles would further enhance the light absorption on the
22 other hand. To further investigate whether rBC concentration or mixing state is more
23 important for determining absorption, the increases in light absorption are compared based on
24 the same percentagewise increment of either rBC mass concentration or number fraction of
25 coated rBC. According to the regression function in Figure 8b and the correlation between
26 absorption and rBC mass (Absorption = $-0.38 + 10.17[rBC]$, $r = 0.92$), the increase of light
27 absorption is larger for number fraction of coated rBC (e.g, Δ light absorption = 1.8 Mm^{-1})
28 than for the rBC mass (e.g, Δ light absorption = 0.5 Mm^{-1}), suggesting that, compared to rBC
29 mass concentration, rBC mixing state is more important in determining absorption during
30 pollution episode.

1 3.4 Implications for direct radiative forcing

2 The direct radiative forcing of BC particles (DRF_{BC}) refers to the change in energy balance at
3 the top of the atmosphere due to absorption and scattering of sunlight by BC particles. Here
4 the DRF_{BC} is estimated from a simple analytical solution derived from the following
5 parameterization (Chylek and Wong, 1995):

$$6 \quad DRF_{BC} = \frac{S_0}{4} T_{atm}^2 \times (1 - N) \times [4\alpha\delta_{ab} - 2 \times (1 - \alpha)^2 \beta\delta_{sc}] \quad (2)$$

7 where S_0 is the solar irradiance (1370 W m^{-2}), T_{atm} is the atmospheric transmission (0.79), N is
8 the cloud fraction (0.6), α is the surface albedo (i.e., 0.18 at rural region), β is the backscatter
9 fraction, which is assumed to be 0.17 (Kim et al., 2012), and δ_{ab} and δ_{sc} are the absorption and
10 scattering optical depth, respectively. The daily values of δ_{ab} and δ_{sc} are estimated from Aura-
11 OMI satellite measurements (<http://disc.sci.gsfc.nasa.gov/>). More details about the
12 assumption of this equation can be found in Kim et al. (2012). The average DRF_{BC} is
13 estimated to be $0.6 \pm 0.4 \text{ W m}^{-2}$ for the entire campaign, ranging from 0.05 to 1.6 W m^{-2} .
14 During rBC pollution episode, the DRF_{BC} was $0.93 \pm 0.57 \text{ W m}^{-2}$, which is about two times
15 higher than that in clean days ($0.48 \pm 0.29 \text{ W m}^{-2}$). It should be noted that the DRF_{BC} is
16 calculated based on the assumption that BC particles are externally mixed with other non-
17 light-absorbing particles. Given that a fraction of BC particles may be internally mixed with
18 other aerosol compounds, the DRF_{BC} calculated here should be considered as the lower limit.
19 Therefore, the BC mediated radiative forcing is of great importance for the local atmospheric
20 radiative balance in the northeastern Qinghai-Tibetan Plateau. Given the much shorter
21 lifetime of BC aerosol compared with greenhouse gases, mitigation of BC pollution could be
22 an efficient control strategy for protecting the vulnerable environment in the Qinghai-Tibetan
23 Plateau because it reduces the radiative forcing directly by reducing the BC particle
24 concentration and indirectly by slowing down the melting of snowpack and ice that can reflect
25 the sunlight. It is worth to note that the rBC concentration during pollution episode was 4
26 times higher than that in clean days, but the DRF_{BC} was only enhanced by a factor of two,
27 suggesting the importance of other aerosol components which made negative contribution to
28 DRF.

1 4 Conclusions

2 The mass concentration, size distribution, mixing state and optical properties of rBC particles
3 in the Qinghai Lake region of the Qinghai-Tibetan Plateau are studied. The results show that
4 average rBC concentration and number fraction of coated rBC are $160 \pm 190 \text{ ng m}^{-3}$ and
5 59.3% , respectively, for the entire campaign in November 2012. The average rBC mass
6 concentration is about 4 times larger for pollution episode than for clean days; and the number
7 fraction of coated rBC particles also increases from 57.758% for clean days to 64.665% for
8 pollution episode. The mass size distribution of rBC particles shows lognormal distribution
9 with a peak diameter of $\sim 187 \text{ nm}$ regardless of the pollution level. Back trajectory analysis
10 and potential source contribution function (PSCF) model study show that North India is an
11 important region influencing the rBC level in the northeastern Qinghai-Tibetan Plateau during
12 the pollution episode. The fire counts map also suggests that the pollution episode is likely
13 caused by biomass burning in North India.

14 The average light absorption (at $\lambda = 532 \text{ nm}$) is 1.3 Mm^{-1} for the clean days and increases to
15 3.7 Mm^{-1} for pollution episode. The rBC mass absorption cross section (MAC_{rBC}) at $\lambda = 532$
16 nm was larger in clean days ($14.9 \text{ m}^2 \text{ g}^{-1}$) than during pollution episode ($9.3 \text{ m}^2 \text{ g}^{-1}$), likely due
17 to the effects of brown carbon and the uncertainty of the MAC_{rBC} calculation. The MAC_{rBC}
18 was positively correlated with number fraction of coated rBC during pollution episode with
19 an increasing rate of $0.18 (\text{m}^2 \text{ g}^{-1}) \%^{-1}$. The number fraction of coated rBC particles shows
20 positive correlation with light absorption, suggesting that the increase of aged rBC particles
21 increases the light absorption. Compared to rBC mass concentration, rBC mixing state is more
22 important in determining absorption during pollution episode, estimated from the same
23 percentagewise increment of either rBC mass concentration or the number fraction of coated
24 rBC . The estimated BC direct radiative forcing is about 2 times higher for pollution episode
25 ($0.93 \pm 0.57 \text{ W m}^{-2}$) than for clean days ($0.48 \pm 0.29 \text{ W m}^{-2}$).

26 This case study provides an insight into the sources, mixing state and optical properties of
27 rBC particles in the northeast Qinghai-Tibetan Plateau.~~South Asia pollution impacting~~
28 ~~northeast Qinghai-Tibetan Plateau through long-range transport.~~ The enhancement of rBC
29 absorption not only disturbs the energy budget of the atmosphere in this region, but also
30 modifies the snow albedo by deposition. This in turn can accelerate the melting of the glaciers
31 and snow-pack over Qinghai-Tibetan and, thus, affect the sustaining seasonal water
32 availability leading to security of agriculture in downstream regions. More studies need to be

1 addressed on the basis of long-period investigations in the Qinghai-Tibetan Plateau region to
2 improve our scientific understanding of the regional climate on the inter-annual as well as
3 intra-seasonal scale.

4 **Acknowledgements**

5 This work was supported by the projects from the National Natural Science Foundation of
6 China (41230641) and the Ministry of Science & Technology (2012BAH31B03, 201209007).

1 **References**

- 2 An, Z., Colman, S.M., Zhou, W., Li, X., Brown, E.T., Jull, A.J.T., Cai, Y., Huang, Y., Lu, X.,
3 Chang, H., Song, Y., Sun, Y., Xu, H., Liu, W., Jin, Z., Liu, X., Cheng, P., Liu, Y., Ai, L.,
4 Li, X., Liu, X., Yan, L., Shi, Z., Wang, X., Wu, F., Qiang, X., Dong, J., Lu, F., Xu, X.:
5 Interplay between the Westerlies and Asian monsoon recorded in Lake Qinghai sediments
6 since 32 ka, *Sci. Rep.*, 2, 619, doi: 10.1038/srep00619, 2012.
- 7 [Andreae, M.O., Gelencser, A.: Black carbon or brown carbon? The nature of light-absorbing](#)
8 [carbonaceous aerosols, *Atmos. Chem. Phys.*, 6, 3131–3148, 2006.](#)
- 9 Anenberg, S.C., Schwartz, J., Shindell, D., Amann, M., Faluvegi, G., Klimont, Z., Janssens-
10 Maenhout, G., Pozzoli, L., Van Dingenen, R., Vignati, E., Emberson, L., Muller, N.Z.,
11 West, J.J., Williams, M., Demkine, V., Hicks, W.K., Kuylensstierna, J., Raes, F.,
12 Ramanathan, V.: Global air quality and health co-benefits of mitigating near-term climate
13 change through methane and black carbon emission controls, *Environ. Health Persp.*, 120,
14 831–839, 2012.
- 15 Bonasoni, P., Laj, P., Marinoni, A., Sprenger, M., Angelini, F., Arduini, J., Bonafe, U.,
16 Calzolari, F., Colombo, T., Decesari, S., Di Biagio, C., di Sarra, A.G., Evangelisti, F.,
17 Duchi, R., Facchini, M.C., Fuzzi, S., Gobbi, G.P., Maione, M., Panday, A., Roccatò, F.,
18 Sellegri, K., Venzac, H., Verza, G.P., Villani, P., Vuillermoz, E., Cristofanelli, P.:
19 Atmospheric Brown Clouds in the Himalayas: first two years of continuous observations at
20 the Nepal Climate Observatory-Pyramid (5079 m), *Atmos. Chem. Phys.*, 10, 7515–7531,
21 2010.
- 22 Bond, T.C. and Bergstrom, R.W.: Light absorption by carbonaceous particles: An
23 investigative review, *Aerosol Sci, Tech.*, 40, 27–67, 2006.
- 24 Bond, T.C., Habib, G., Bergstrom, R.W.: Limitations in the enhancement of visible light
25 absorption due to mixing state, *J. Geophys. Res.*, 111, D20211, doi:
26 10.1029/2006JD007315, 2006.
- 27 Bond, T.C., Doherty, S.J., Fahey, D.W., Forster, P.M., Berntsen, T., DeAngelo, B.J., Flanner,
28 M.G., Ghan, S., Kärcher, B., Koch, D., Kinne, S., Kondo, Y., Quinn, P.K., Sarofim, M.C.,
29 Schultz, M.G., Schulz, M., Venkataraman, C., Zhang, H., Zhang, S., Bellouin, N.,
30 Guttikunda, S.K., Hopke, P.K., Jacobson, M.Z., Kaiser, J.W., Klimont, Z., Lohmann, U.,
31 Schwarz, J.P., Shindell, D., Storelvmo, T., Warren, S.G., Zender, C.S.: Bounding the role

1 of black carbon in the climate system: A scientific assessment, *J. Geophys. Res.*, 118,
2 5380–5552, 2013.

3 [Browne, E.C., Franklin, J.P., Canagaratna, M.R., Massoli, P., Kirchstetter, T.W., Worsnop,](#)
4 [D.R., Wilson, K.R., Kroll, J.H.: Changes to the chemical composition of soot from](#)
5 [heterogeneous oxidation reactions, *J. Phys. Chem. A*, 119, 1154–1163, 2015.](#)

6 Cao, J.J., Tie, X.X., Xu, B.Q., Zhao, Z.Z., Zhu, C.S., Li, G.H., Liu, S.X.: Measuring and
7 modeling black carbon (BC) contamination in the SE Tibetan Plateau, *J. Atmos. Chem.*, 67,
8 45–60, 2010.

9 [Cheng, Y.F., Eichler, H., Wiedensohler, A., Heintzenberg, J., Zhang, Y.H., Hu, M., Herrmann,](#)
10 [H., Zeng, L.M., Liu, S., Gnauk, T., Brüggemann, E., He, L.Y.: Mixing state of elemental](#)
11 [carbon and non-light-absorbing aerosol components derived from in situ particle optical](#)
12 [properties at Xinken in Pearl River Delta of China, *J. Geophys. Res.*, 111, D20204, doi:](#)
13 [10.1029/2005JD006929, 2006.](#)

14 [Cheng, Y., Su, H., Rose, D., Gunthe, S., Berghof, M., Wehner, B., Achtert, P., Nowak, A.,](#)
15 [Takegawa, N., and Kondo, Y.: Size-resolved measurement of the mixing state of soot in the](#)
16 [megacity Beijing, China: diurnal cycle, aging and parameterization, *Atmos. Chem. Phys.*,](#)
17 [12, 4477–4491, 2012.](#)

18 ~~Cape, J.N., Coyle, M., Dumitrescu, P.: The atmospheric lifetime of black carbon, *Atmos.*
19 ~~*Environ.*, 59, 256–263, 2012.~~~~

20 Chung, C.E., Lee, K., Mueller, D.: Effect of internal mixture on black carbon radiative
21 forcing, *Tellus B*, 64, 1–13, 2012.

22 ~~Chung, S.H. and Seinfeld, J.H.: Climate response of direct radiative forcing of anthropogenic~~
23 ~~black carbon, *J. Geophys. Res.*, 110, D11102, doi:10.1029/2004JD005441, 2005.~~

24 Chylek, P. and Wong, J.: Effect of absorbing aerosols on global radiation budget, *Geophys.*
25 *Res. Lett.*, 22, 929–931, 1995.

26 Collaud Coen, M., Weingartner, E., Apituley, A., Ceburnis, D., Fierz-Schmidhauser, R.,
27 Flentje, H., Henzing, J., Jennings, S.G., Moerman, M., Petzold, A.: Minimizing light
28 absorption measurement artifacts of the Aethalometer: evaluation of five correction
29 algorithms, *Atmos. Meas. Tech.*, 3, 457–474, 2010.

- 1 Cong, Z., Kang, S., Gao, S., Zhang, Y., Li, Q., Kawamura, K.: Historical trends of
2 atmospheric black carbon on Tibetan Plateau as reconstructed from a 150-Year lake
3 sediment record, *Environ. Sci. Technol.*, 47, 2579–2586, 2013.
- 4 Forbes, M.S., Raison, R.J., Skjemstad, J.O.: Formation, transformation and transport of black
5 carbon (charcoal) in terrestrial and aquatic ecosystems, *Sci. Total Environ.*, 370, 190–206,
6 2006.
- 7 ~~Fuller, K.A., Malm, W.C., Kreidenweis, S.M.: Effects of mixing on extinction by
8 carbonaceous particles, *J. Geophys. Res.*, 104, 15941–15954, 1999.~~
- 9 Gao, R., Schwarz, J., Kelly, K., Fahey, D., Watts, L., Thompson, T., Spackman, J., Slowik, J.,
10 Cross, E., Han, J.H.: A novel method for estimating light-scattering properties of soot
11 aerosols using a modified single-particle soot photometer, *Aerosol Sci, Tech.*, 41, 125–135,
12 2007.
- 13 ~~Hansen, J., Sato, M., Ruedy, R., Nazarenko, L., Lacis, A., Schmidt, G.A., Russell, G.,
14 Aleinov, I., Bauer, M., Bauer, S., Bell, N., Cairns, B., Canuto, V., Chandler, M., Cheng, Y.,
15 Del-Genio, A., Faluvegi, G., Fleming, E., Friend, A., Hall, T., Jackman, C., Kelley, M.,
16 Kiang, N., Koch, D., Lean, J., Lerner, J., Lo, K., Menon, S., Miller, R., Minnis, P.,
17 Novakov, T., Oinas, V., Perlwitz, J., Rind, D., Romanou, A., Shindell, D., Stone, P., Sun,
18 S., Tausnev, N., Thresher, D., Wielicki, B., Wong, T., Yao, M., Zhang, S.: Efficacy of
19 climate forcings, *J. Geophys. Res.*, 110, D18104, doi: 10.1029/2005JD005776, 2005.~~
- 20 Heo, J., McGinnis, J.E., de Foy, B., Schauer, J.J.: Identification of potential source areas for
21 elevated PM_{2.5}, nitrate and sulfate concentrations, *Atmos. Environ.*, 71, 187–197, 2013.
- 22 Hindman, E.E. and Upadhyay, B.P.: Air pollution transport in the Himalayas of Nepal and
23 Tibet during the 1995-1996 dry season, *Atmos. Environ.*, 36, 727–739, 2002.
- 24 Immerzeel, W.W., van Beek, L.P.H., Bierkens, M.F.P.: Climate change will affect the Asian
25 water towers, *Science*, 328, 1382–1385, 2010.
- 26 Jacobson, M.Z.: Strong radiative heating due to the mixing state of black carbon in
27 atmospheric aerosols, *Nature*, 409, 695–697, 2001.
- 28 Kühn, T., Partanen, A.I., Laakso, A., Lu, Z., Bergman, T., Mikkonen, S., Kokkola, H.,
29 Korhonen, H., Räisänen, P., Streets, D.G., Romakkaniemi, S., Laaksonen, A.: Climate

- 1 impacts of changing aerosol emissions since 1996, *Geophys. Res. Lett.*, 41, 4711–4718,
2 2014.
- 3 Kim, M.Y., Lee, S.-B., Bae, G.-N., Park, S.S., Han, K.M., Park, R.S., Song, C.H., Park, S.H.:
4 Distribution and direct radiative forcing of black carbon aerosols over Korean Peninsula,
5 *Atmos. Environ.*, 58, 45–55, 2012.
- 6 [Koch, D. and Del Genio, A. D.: Black carbon semi-direct effects on cloud cover: review and](#)
7 [synthesis, *Atmos. Chem. Phys.*, 10, 7685–7696, 2010.](#)
- 8 Kondo, Y., Matsui, H., Moteki, N., Sahu, L., Takegawa, N., Kajino, M., Zhao, Y., Cubison,
9 M. J., Jimenez, J. L., Vay, S., Diskin, G. S., Anderson, B., Wisthaler, A., Mikoviny, T.,
10 Fuelberg, H. E., Blake, D. R., Huey, G., Weinheimer, A. J., Knapp, D. J., Brune, W. H.:
11 Emissions of black carbon, organic, and inorganic aerosols from biomass burning in North
12 America and Asia in 2008, *J. Geophys. Res.*, 116(D8), D08204,
13 doi:10.1029/2010JD015152, 2011.
- 14 Kopacz, M., Mauzerall, D.L., Wang, J., Leibensperger, E.M., Henze, D.K., Singh, K.: Origin
15 and radiative forcing of black carbon transported to the Himalayas and Tibetan Plateau,
16 *Atmos. Chem. Phys.*, 11, 2837–2852, 2011.
- 17 Kurokawa, J., Ohara, T., Morikawa, T., Hanayama, S., Janssens-Maenhout, G., Fukui, T.,
18 Kawashima, K., Akimoto, H.: Emissions of air pollutants and greenhouse gases over Asian
19 regions during 2000–2008: Regional emission inventory in ASia (REAS) version 2, *Atmos.*
20 *Chem. Phys.*, 13, 11019–11058, 2013.
- 21 ~~[Lack, D. and Cappa, C.: Impact of brown and clear carbon on light absorption enhancement,](#)~~
22 ~~[single scatter albedo and absorption wavelength dependence of black carbon, *Atmos.*](#)~~
23 ~~[*Chem. Phys.*, 10, 4207–4220, 2010.](#)~~
- 24 [Liu, D., Allan, J., Whitehead, J., Young, D., Flynn, M., Coe, H., McFiggans, G., Fleming,](#)
25 [Z.L., Bandy, B.: Ambient black carbon particle hygroscopic properties controlled by](#)
26 [mixing state and composition, *Atmos. Chem. Phys.*, 13, 2015–2029, 2013.](#)
- 27 Lohmann, U. and Feichter, J.: Global indirect aerosol effects: a review, *Atmos. Chem. Phys.*,
28 5, 715–737, 2005.
- 29 Lu, Z., Streets, D.G., Zhang, Q., Wang, S.: A novel back-trajectory analysis of the origin of
30 black carbon transported to the Himalayas and Tibetan Plateau during 1996–2010, *Geophys.*
31 *Res. Lett.*, 39, L01809, doi: 10.1029/2011GL049903, 2012.

- 1 McMeeking, G., Morgan, W., Flynn, M., Highwood, E., Turnbull, K., Haywood, J., Coe, H.:
2 Black carbon aerosol mixing state, organic aerosols and aerosol optical properties over the
3 United Kingdom, *Atmos. Chem. Phys.*, 11, 9037–9052, 2011.
- 4 Ming, J., Wang, P., Zhao, S., Chen, P.: Disturbance of light-absorbing aerosols on the albedo
5 in a winter snowpack of Central Tibet, *J. Environ. Sci.*, 25, 1601–1607, 2013.
- 6 Moteki, N. and Kondo, Y.: Effects of mixing state on black carbon measurements by laser-
7 induced incandescence, *Aerosol Sci, Tech.*, 41, 398–417, 2007.
- 8 Perring, A., Schwarz, J., Spackman, J., Bahreini, R., de Gouw, J., Gao, R., Holloway, J., Lack,
9 D., Langridge, J., Peischl, J.: Characteristics of black carbon aerosol from a surface oil burn
10 during the Deepwater Horizon oil spill, *Geophys. Res. Lett.*, 38, L17809, doi:
11 10.1029/2011GL048356, 2011.
- 12 [Ping, X., Jiang, Z., Li, C.: Status and future perspectives of energy consumption and its
13 ecological impacts in the Qinghai-Tibet region, *Renew. Sustain Energy Rev.*, 15, 514–523,
14 2011.](#)
- 15 ~~Polissar, A.V., Hopke, P.K., Harris, J.M.: Source regions for atmospheric aerosol measured at
16 Barrow, Alaska, *Environ. Sci. Technol.*, 35, 4214–4226, 2001.~~
- 17 Polissar, A.V., Hopke, P.K., Paatero, P., Kaufmann, Y.J., Hall, D.K., Bodhaine, B.A., Dutton,
18 E.G., Harris, J.M.: The aerosol at Barrow, Alaska: long-term trends and source locations,
19 *Atmos. Environ.*, 33, 2441–2458, 1999.
- 20 [Polissar, A.V., Hopke, P.K., Harris, J.M.: Source regions for atmospheric aerosol measured at
21 Barrow, Alaska, *Environ. Sci. Technol.*, 35, 4214–4226, 2001.](#)
- 22 Ramanathan, V. and Carmichael, G.: Global and regional climate changes due to black carbon,
23 *Nat. Geosci.*, 1, 221–227, 2008.
- 24 [Riemer, N., West, M., Zaveri, R., Easter, R.: Estimating black carbon aging time-scales with
25 a particle-resolved aerosol model, *J. Aerosol Sci.*, 41, 143–158, 2010.](#)
- 26 [Rose, D., Gunthe, S., Su, H., Garland, R., Yang, H., Berghof, M., Cheng, Y., Wehner, B.,
27 Achtert, P., and Nowak, A.: Cloud condensation nuclei in polluted air and biomass burning
28 smoke near the mega-city Guangzhou, China–Part 2: Size-resolved aerosol chemical
29 composition, diurnal cycles, and externally mixed weakly CCN-active soot particles,
30 *Atmos. Chem. Phys.*, 11, 2817–2836, 2011.](#)

- 1 Sahu, S.K., Beig, G., Sharma, C.: Decadal growth of black carbon emissions in India,
2 Geophys. Res. Lett., 35, L02807, doi: 10.1029/2007GL032333, 2008.
- 3 [Sahu, L.K., Kondo, Y., Moteki, N., Takegawa, N., Zhao, Y., Cubison, M. J., Jimenez, J. L.,
4 Vay, S., Diskin, G. S., Wisthaler, A., Mikoviny, T., Huey, L. G., Weinheimer, A. J. and
5 Knapp, D. J.: Emission characteristics of black carbon in anthropogenic and biomass
6 burning plumes over California during ARCTAS-CARB 2008, J. Geophys. Res., 117\(D16\),
7 D16302, doi:10.1029/2011JD017401, 2012.](#)
- 8 Schwarz, J.P., Gao, R.S., Fahey, D.W., Thomson, D.S., Watts, L.A., Wilson, J.C., Reeves,
9 J.M., Darbeheshti, M., Baumgardner, D.G., Kok, G.L., Chung, S.H., Schulz, M., Hendricks,
10 J., Lauer, A., Kärcher, B., Slowik, J.G., Rosenlof, K.H., Thompson, T.L., Langford, A.O.,
11 Loewenstein, M., Aikin, K.C.: Single-particle measurements of midlatitude black carbon
12 and light-scattering aerosols from the boundary layer to the lower stratosphere, J. Geophys.
13 Res., 111, D16207, doi: 10.1029/2006JD007076, 2006.
- 14 Schwarz, J.P., Gao, R.S., Spackman, J.R., Watts, L.A., Thomson, D.S., Fahey, D.W., Ryerson,
15 T.B., Peischl, J., Holloway, J.S., Trainer, M., Frost, G.J., Baynard, T., Lack, D.A., de Gouw,
16 J.A., Warneke, C., Del Negro, L.A.: Measurement of the mixing state, mass, and optical
17 size of individual black carbon particles in urban and biomass burning emissions, Geophys.
18 Res. Lett., 35, L13810, doi: 10.1029/2008GL033968, 2008a.
- 19 ~~Schwarz, J.P., Spackman, J.R., Fahey, D.W., Gao, R.S., Lohmann, U., Stier, P., Watts, L.A.,
20 Thomson, D.S., Lack, D.A., Pfister, L., Mahoney, M.J., Baumgardner, D., Wilson, J.C.,
21 Reeves, J.M.: Coatings and their enhancement of black carbon light absorption in the
22 tropical atmosphere, J. Geophys. Res., 113, D03203, doi: 10.1029/2007JD009042, 2008b.~~
- 23 Schwarz, J.P., Spackman, J.R., Gao, R.S., Watts, L.A., Stier, P., Schulz, M., Davis, S.M.,
24 Wofsy, S.C., Fahey, D.W.: Global-scale black carbon profiles observed in the remote
25 atmosphere and compared to models, Geophys. Res. Lett., 37, L18812, doi:
26 10.1029/2010GL044372, 2010.
- 27 Seinfeld, J.H. and Pandis, S.N.: Atmospheric chemistry and physics: From air pollution to
28 climate change, Wiley, New York, 1998.
- 29 Shiraiwa, M., Kondo, Y., Iwamoto, T., Kita, K.: Amplification of light absorption of black
30 carbon by organic coating, Aerosol Sci, Tech., 44, 46–54, 2010.

- 1 Slowik, J.G., Cross, E.S., Han, J.H., Davidovits, P., Onasch, T.B., Jayne, J.T., Williams, L.R.,
2 Canagaratna, M.R., Worsnop, D.R., Chakrabarty, R.K.: An inter-comparison of instruments
3 measuring black carbon content of soot particles, *Aerosol Sci, Tech.*, 41, 295–314, 2007.
- 4 Stephens, M., Turner, N., Sandberg, J.: Particle identification by laser-induced incandescence
5 in a solid-state laser cavity, *Appl. Optics*, 42, 3726–3736, 2003.
- 6 Su, F., Duan, X., Chen, D., Hao, Z., Cuo, L.: Evaluation of the Global Climate Models in the
7 CMIP5 over the Tibetan Plateau, *J. Climate*, 26, 3187–3208, 2013.
- 8 [Taylor, J. W., Allan, J. D., Allen, G., Coe, H., Williams, P. I., Flynn, M. J., Le Breton, M.,
9 Muller, J. B. A., Percival, C. J., Oram, D., Forster, G., Lee, J. D., Rickard, A. R., Parrington,
10 M., and Palmer, P. I.: Size-dependent wet removal of black carbon in Canadian biomass
11 burning plumes, *Atmos. Chem. Phys.*, 14, 13755-13771, 2014.](#)
- 12 [Taylor, J. W., Allan, J. D., Liu, D., Flynn, M., Weber, R., Zhang, X., Lefer, B. L., Grossberg,
13 N., Flynn, J., Coe, H.: Assessment of the sensitivity of core/shell parameters derived using
14 the single-particle soot photometer to density and refractive index, *Atmos. Meas. Tech.*,
15 8\(4\), 1701–1718, 2015.](#)
- 16 Tollefsen, P., Rypdal, K., Torvanger, A., Rive, N.: Air pollution policies in Europe:
17 Efficiency gains from integrating climate effects with damage costs to health and crops,
18 *Environ. Sci. Policy*, 12, 870–881, 2009.
- 19 [Wan, X., Kang, S., Wang, Y., Xin, J., Liu, B., Guo, Y., Wen, T., Zhang, G., and Cong, Z.:
20 Size distribution of carbonaceous aerosols at a high-altitude site on the central Tibetan
21 Plateau \(Nam Co Station, 4730 m a.s.l.\), *Atmos. Res.*, 153, 155-164, 2015.](#)
- 22 Wang, Q.Y., Schwarz, J.P., Cao, J.J., Gao, R.S., Fahey, D.W., Hu, T.F., Huang, R.-J., Han,
23 Y.M., Shen, Z.X.: Black carbon aerosol characterization in a remote area of Qinghai–
24 Tibetan Plateau, western China, *Sci. Total Environ.*, 479, 151–158, 2014a.
- 25 Wang, Q.Y., Huang, R.-J., Cao, J.J., Han, Y.M., Wang, G.H., Li, G.H., Wang, Y.C., Dai,
26 W.T., Zhang, R.J., Zhou, Y.Q.: Mixing state of black carbon aerosol in a heavily polluted
27 urban area of China: Implications for light absorption enhancement, *Aerosol Sci, Tech.*, 48,
28 689–697, 2014b.

- 1 [Wang, Q., Liu, S., Zhou, Y., Cao, J., Han, Y., Ni, H., Zhang, N., Huang, R.: Characteristics of](#)
2 [black carbon aerosol during the Chinese Lunar Year and weekdays in Xi'an, China,](#)
3 [Atmosphere, 6, 195–208, 2015.](#)
- 4 Wang, Y.Q., Zhang, X.Y., Arimoto, R.: The contribution from distant dust sources to the
5 atmospheric particulate matter loadings at XiAn, China during spring, *Sci. Total Environ.*,
6 368, 875–883, 2006.
- 7 Watson, J.G., Chow, J.C., Chen, L.W.A.: Summary of organic and elemental carbon/black
8 carbon analysis methods and intercomparisons, *Aerosol Air Qual. Res.*, 5, 65–102, 2005.
- 9 Wild, M., Ohmura, A., Makowski, K.: Impact of global dimming and brightening on global
10 warming, *Geophys. Res. Lett.*, 34, L04702, doi: 10.1029/2006GL028031, 2007.
- 11 Xia, X., Zong, X., Cong, Z., Chen, H., Kang, S., Wang, P.: Baseline continental aerosol over
12 the central Tibetan plateau and a case study of aerosol transport from South Asia, *Atmos.*
13 *Environ.*, 45, 7370–7378, 2011.
- 14 Xu, B., Cao, J., Joswiak, D.R., Liu, X., Zhao, H., He, J.: Post-depositional enrichment of
15 black soot in snow-pack and accelerated melting of Tibetan glaciers, *Environ. Res. Lett.*, 7,
16 014022, doi:10.1088/1748-9326/7/1/014022, 2012.
- 17 Xu, B., Cao, J., Hansen, J., Yao, T., Joswia, D.R., Wang, N., Wu, G., Wang, M., Zhao, H.,
18 Yang, W.: Black soot and the survival of Tibetan glaciers, *P. Natl. Acad. Sci. USA*, 106,
19 22114–22118, 2009.
- 20 Yang, K., Wu, H., Qin, J., Lin, C., Tang, W., Chen, Y.: Recent climate changes over the
21 Tibetan Plateau and their impacts on energy and water cycle: A review, *Global Planet.*
22 *Change*, 112, 79–91, 2014.
- 23 Yang, M., Howell, S.G., Zhuang, J., Huebert, B.J.: Attribution of aerosol light absorption to
24 black carbon, brown carbon, and dust in China-interpretations of atmospheric
25 measurements during EAST-AIRE, *Atmos. Chem. Phys.*, 9, 2035–2050, 2009.
- 26 Zhang, Q., Streets, D.G., Carmichael, G.R., He, K.B., Huo, H., Kannari, A., Klimont, Z., Park,
27 I.S., Reddy, S., Fu, J.S.: Asian emissions in 2006 for the NASA INTEX-B mission, *Atmos.*
28 *Chem. Phys.*, 9, 5131–5153, 2009.

- 1 Zhang, R., Jing, J., Tao, J., Hsu, S.C., Wang, G., Cao, J., Lee, C.S.L., Zhu, L., Chen, Z., Zhao,
2 Y., Shen, Z.: Chemical characterization and source apportionment of PM_{2.5} in Beijing:
3 seasonal perspective, *Atmos. Chem. Phys.*, 13, 7053–7074, 2013.
- 4 Zhao, S., Ming, J., Sun, J., Xiao, C.: Observation of carbonaceous aerosols during 2006–2009
5 in Nyainqêntanglha Mountains and the implications for glaciers, *Environ. Sci. Pollut. R.*,
6 20, 5827–5838, 2013.
- 7 Zhuang, B.L., Li, S., Wang, T.J., Deng, J.J., Xie, M., Yin, C.Q., Zhu, J.L.: Direct radiative
8 forcing and climate effects of anthropogenic aerosols with different mixing states over
9 China, *Atmos. Environ.*, 79, 349–361, 2013.

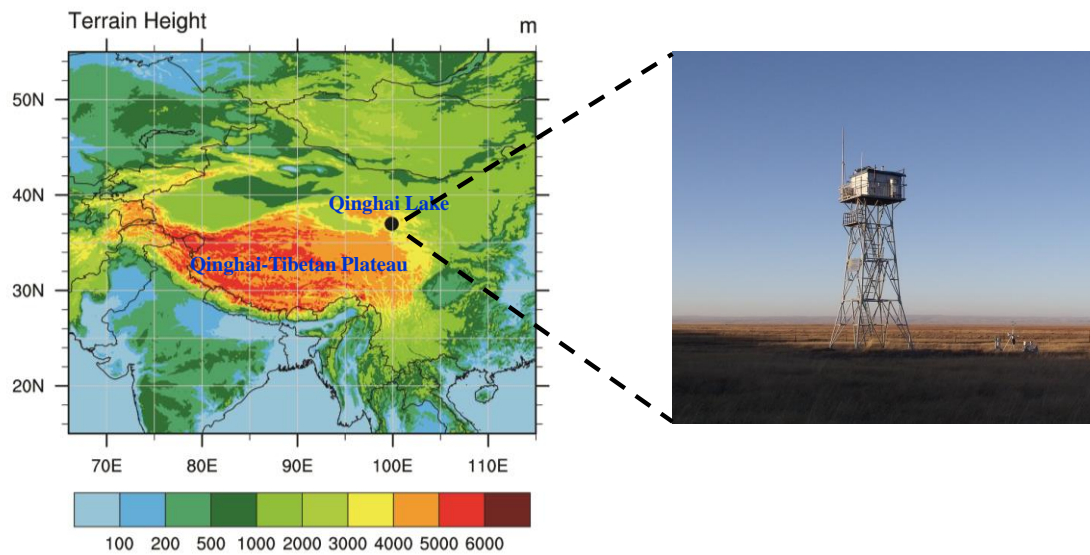
1 | Table 1 Summary of rBC concentrations, number fraction of coated rBC, light absorption coefficient, and mass absorption cross section of
 2 | rBC (MAC_{rBC}) during different sampling periods.

	rBC (mean ± SD, ng m ⁻³)			Number fraction of coated rBC (%)			Absorption (Mm ⁻¹)			MAC _{rBC} (m ² g ⁻¹)		
	PE [*]	CD [*]	All	PE	CD	All	PE	CD	All	PE	CD	All
Average	390±207	86±101	160±190	65±5	58±7	59±7	3.7±2.9	1.3±1.6	2.1±2.4	9.3±3.1	14.9±8.9	13.2±8.1
25th	219	40	50	63	53	54	1.4	0.7	0.8	7.4	9.0	8.3
50th	410	68	80	66	58	60	3.4	0.9	1.2	9.0	13.6	11.2
75th	489	103	170	68	63	65	4.4	1.4	2.0	10.7	18.7	16.7

4 | ^{*}PE and CD represent the pollution episode and clean days, respectively.

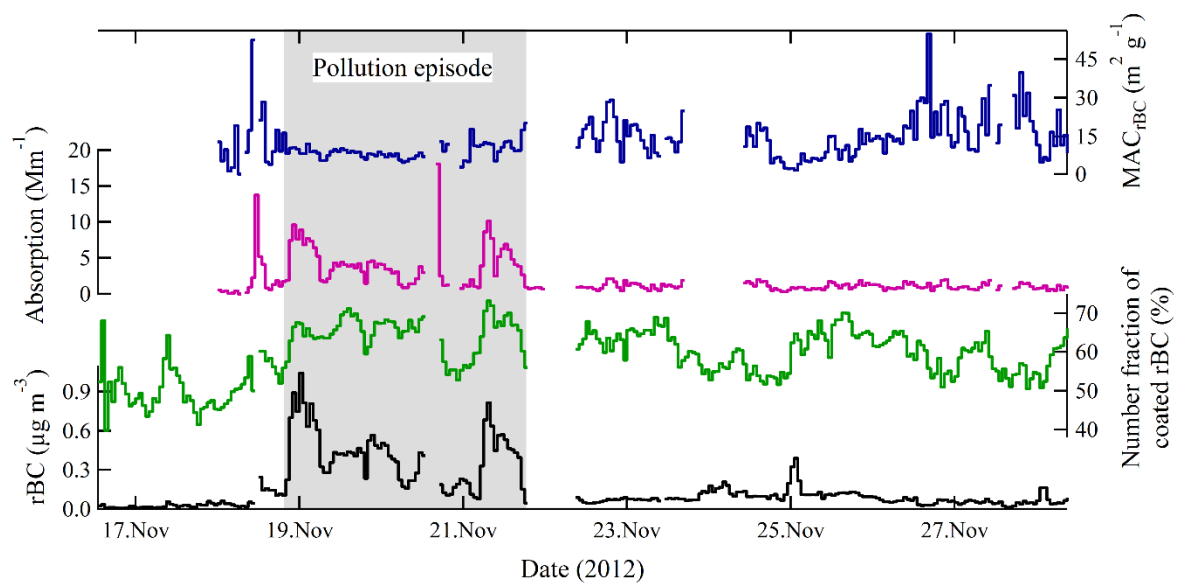
5

6



1
2
3
4
5
6

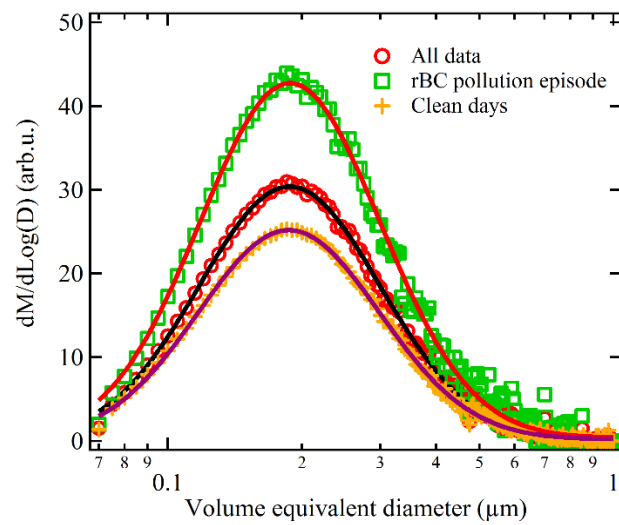
Figure 1. (left) Geographical location of Qinghai-Tibetan Plateau and surrounding areas. Color code represents topographical features (unit: m). (right) Observation tower at the “Bird Island” peninsula in Qinghai Lake, China.



1
2
3
4
5
6
7
8
9
10
11
12
13
14
15
16
17
18

Figure 2. Time series of the rBC mass concentration, number fraction of coated rBC, light absorption at $\lambda = 532 \text{ nm}$, and mass absorption cross section of rBC (MAC_{rBC}) during the entire campaign period. The pollution episode is highlighted with grey background.

1



2

3

4 | Figure 3. Mass size distribution of rBC in volume equivalent diameter during different
5 | sampling periods at Qinghai Lake. The solid lines represent lognormal fit. “M” and “D” in
6 | vertical label represent rBC mass and void free diameter (assuming 2 g cm^{-3} density),
7 | respectively.

8

9

10

11

12

13

14

15

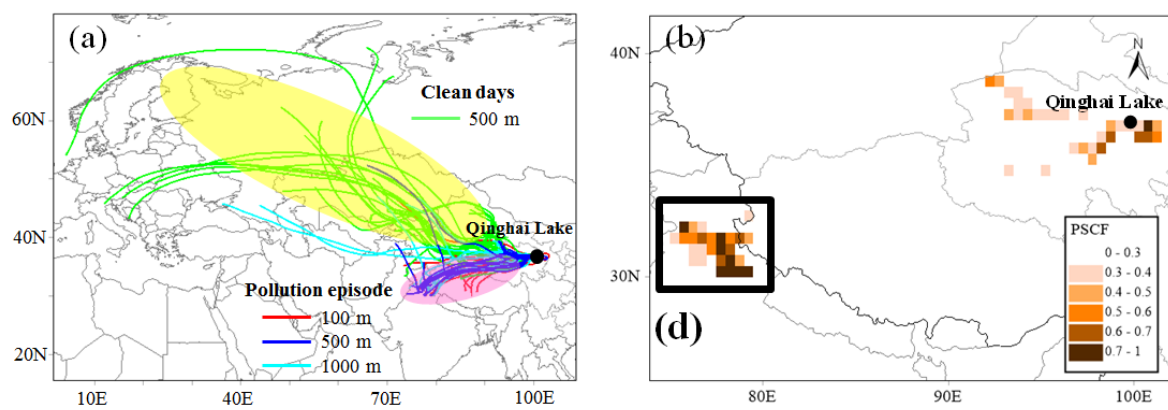
16

17

18

19

1



2

3

4 Figure 4. (a) Five-day backward air mass trajectories reaching at Qinghai Lake at 100, 500
5 and 1000 m above ground every six hours and (b) Likely source areas of rBC identified using
6 potential source contribution function (PSCF) plots during the entire campaign.

7

8

9

10

11

12

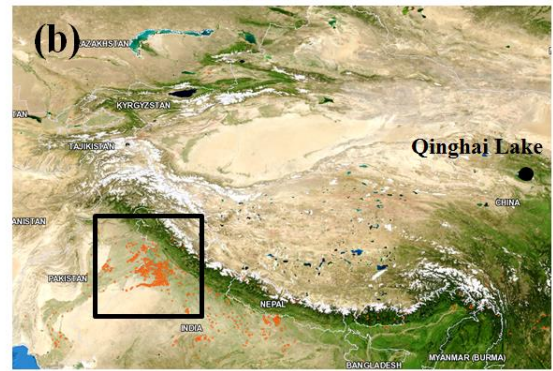
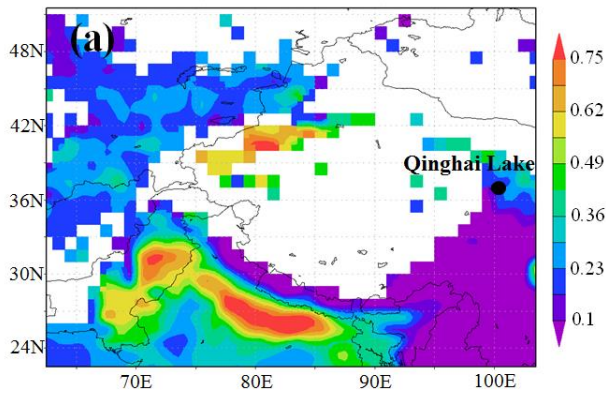
13

14

15

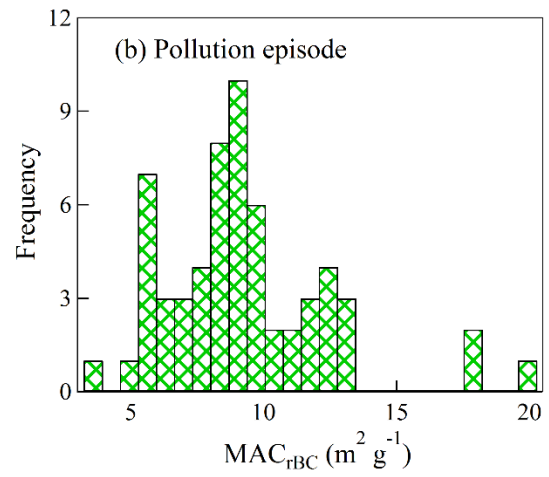
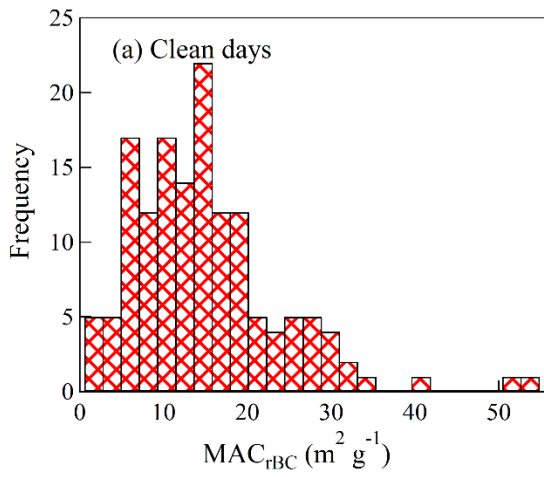
16

17



1
2
3
4
5
6
7
8
9
10
11
12
13
14
15

Figure 5. Regional distributions of (a) aerosol optical depth (AOD) and (b) fire counts map over Qinghai-Tibetan Plateau derived from MODIS observation during 16–27 November, 2012.



1

2

3 Figure 6. Frequency distributions of rBC mass absorption cross section (MAC_{rBC}) during (a)
 4 clean days and (b) pollution episode.

5

6

7

8

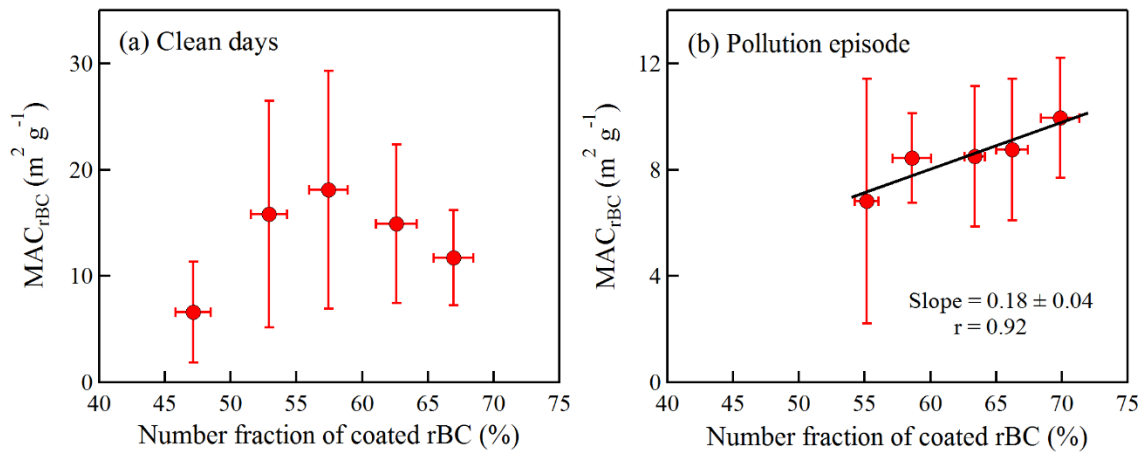
9

10

11

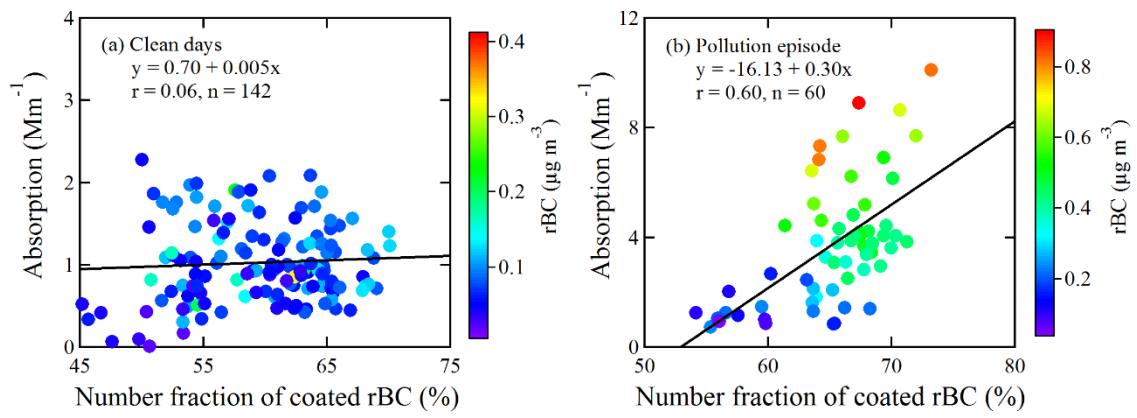
12

13



1
2
3
4
5
6
7
8
9
10
11
12
13
14

Figure 7. Mass absorption cross section of rBC (MAC_{rBC}) versus number fraction of coated rBC during (a) clean days and (b) pollution episode. The error bars correspond to the standard deviations of MAC_{rBC} and number fraction of coated rBC.



1
 2
 3
 4
 5

Figure 8. Light absorption as a function of number fraction of coated rBC during (a) clean days and (b) pollution episode. Data points are color coded for rBC mass concentration.